CHEMISTRY
A EUROPEAN JOURNAL

DOI: 10.1002/chem.200500487

Structural, Electronic, and Bonding Properties of Zeolite Sn-Beta: A Periodic Density Functional Theory Study

Sharan Shetty,[a] Sourav Pal,*[a] Dilip G. Kanhere,[b] and Annick Goursot[c]

Abstract: The structural, electronic, and the bonding properties of the zeolite Sn-beta (Sn-BEA) have been investigated by using the periodic density functional theory. Each of the nine different T-sites in BEA were substituted by Sn atoms and all the nine geometries were completely optimized by using the plane-wave basis set in conjunction with the ultra-soft pseudopotential. On the basis of the structural and the electronic properties, it has been demonstrated that the substitution of Sn atoms in the BEA framework is an endothermic process and hence the incorporation of Sn in the BEA is limited. The lowest unoccupied molecular orbitals (LUMO) energies have been used to characterize the Lewis acidity of each T-site. On the basis of the relative cohesive energy and the LUMO energy, the T2 site is shown to be the most favorable site for the substitution Sn atoms in the BEA framework.

Keywords: cohesive energy · density functional calculations · tin · zeolites

Introduction

Zeolite beta (BEA) was synthesized in 1967 and showed high catalytic activity.[1] The structure of BEA was only recently determined, because crystals of BEA always contain severe structure faulting and hence lead to strong diffuse scattering in diffraction patterns. In 1988 Newsam et al.,[2] succeeded in solving the structure mainly with the use of electron microscopy. They showed that the structure of BEA consists of an intergrown hybrid of two distinct polytypic series of layers, namely, polymorphs A and B. Both the polymorphs have three-dimensional networks of 12-ring pores. The polymorph grows as two-dimensional sheets and the sheets randomly alternate between the two. Very recently polymorph C has been proposed by Corma et al.[3] BEA has two mutually perpendicular straight channels each with a cross section of 0.76×0.64 nm along the *a* and *b* directions and a helical channel of 0.55×0.55 nm along the *c* axis. BEA is of great industrial interest because of its high acidity and larger pore size.[4] BEA has been successfully used for acid-catalyzed reactions,[5] catalytic cracking, [6] and aromatic and aliphatic alkylation.[7] It has been shown that the acidity of BEA can be tuned by the incorporation of tri- and tetravalent atoms (B, Al, V, Ti, Sn, Cr, Fe) into the framework positions.[8–13] The isomorphous substitution creates various Brønsted and Lewis acid sites in BEA. It has been shown in the earlier studies that Brønsted acid sites are present both in the internal and external surfaces.[13] However, this is not true for the Lewis acid sites. They are predominantly present in the framework.[13] The nature of the acid sites created by the isomorphous substitution plays a crucial role in understanding some important oxidation and reduction reactions.[11–20] Interestingly NMR studies have been used to characterize the nature and the acidity of various active sites in BEA.[16,17] Valerio et al. have correlated the ^{29}Si NMR signals with the Si-O-Si bond angles in BEA.[17] They further showed that the nine T-sites in BEA belong to three categories, as follows; sites T7, T8, T9 are associated with no four-membered rings, T1 and T2 are associated with one four-membered ring and T3, T4, T5, T6 are associated with two four-membered rings.[17]

Recently, Sn-BEA was shown to have better catalytic activity than Ti-BEA.[8] Al-free-Sn BEA was first synthesized by Mal and Ramaswamy, who predicted that the Sn atom should be tetrahedrally coordinated.[21] Corma et al. showed for the first time that the Sn-BEA acts as an efficient cata-

[a] S. Shetty, Dr. S. Pal
Theoretical Chemistry Group, Physical Chemistry Division
National Chemical Laboratory, Pune-411008 (India)
Fax: (+91) 202-589-3044
E-mail: pal@ems.ncl.res.in

[b] D. G. Kanhere
Centre for Modeling and Simulation and Department of Physics
University of Pune, Pune-411008 (India)

[c] A. Goursot
Ecole de Chemie e Montpellier
UMR 5618 CNRS Ecole de Chemie, 8, rue de l'Ecole
Normale 34296, Montpellier, Cedex 5 (France)

lyst for the Baeyer–Villiger oxidation reaction in the presence of H_2O_2.[8] They further showed the probable reaction mechanism of the Baeyer–Villiger oxidation reaction, in which the carbonyl group of the ketone is initially activated, and then followed by a reaction with the nonactivated H_2O_2, in contrast to what occurs in the Ti-BEA zeolite.[8] Later, it was also shown by Corma et al., that Sn-BEA acts as a better catalyst than the Ti-BEA for the MPVO reaction.[22,23] The increase in the activity of BEA by the substitution of Sn can be rationalized by the higher atomic size and electronegativity than the Ti atom, giving rise to stronger Lewis acid sites. This shows that the combined property of large pore dimension and high Lewis acidity of Sn-BEA makes it a highly active stereoselective catalyst for many oxidation and reduction reactions. The Sn^{119} MAS NMR spectrum of Sn-BEA confirmed that the Sn atoms have a tetrahedral rather than octahedral coordination.[22–24] This was also attributed to the Sn active sites present within the framework, but not on the external surface in the form of SnO_2.[24] It has been shown that the substitution of Si by a Ti atom in the zeolite framework always results in an increase of the cell volume.[25] It is known that the crystallographically inequivalent T-sites will have different activity and shape selectivity due to the differences in the topological environment around the T-sites. Hence, in the isomorphically substituted zeolites such as Sn-BEA and Ti-BEA, it is important to understand the nature of the active sites and to precise their structures. Experimental techniques such as X-ray diffraction, and magic-angle-spinning (MAS) NMR and IR spectroscopy have been used to investigate the coordination of the active T-sites in the zeolite and their interaction with organic molecules.[23,24,26,27] However, in zeolites such as Sn-BEA or Ti-BEA, in which the concentration of the Sn or Ti is low in the framework, it becomes difficult to obtain the structural features of the local active sites by using these experimental techniques.[24,26]

Various quantum-mechanical methods have been implemented to study the structural and electronic properties of the active sites in zeolites. Finite or cluster models of an active site cut out of the zeolite crystal have been used for theoretical investigations, in which the dangling bonds of the cluster are saturated by hydrogen atoms. The reviews by Sauer and co-workers may be referred for detailed study on the cluster models of zeolites.[28,29] The advantage of using the cluster model is that it avoids artificial periodicity for systems with large Al and cation content and is computationally cheap. It is also a better model for representing the active sites on the surface. However, cluster models neglect the effect of long-range interactions and some artificial states are introduced due to the atoms lying at the boundary of the truncated fragment. Periodic methods are the only way to overcome all these problems, as they include the long-range electrostatic interactions. Studies on the comparison of clusters versus the periodic calculations have been carried out in past.[29,30]

Sastre and Corma have carried out cluster calculations on the Ti-BEA and TS-1 using ab initio Hartree–Fock and density functional theory.[31] On the basis of the LUMO energies, they characterized the acidity of these two zeolites and proved that Ti-BEA is more Lewis acidic than TS-1.[31] Dimitrova and Popova have done a cluster study of Al, B, Ti, and V incorporated into BEA and further studied their interaction with the peroxo group (O–O–H).[32] They showed that the incorporation of Ti is energetically more favorable than the other atoms and Ti increases the oxidizing power of the peroxo group. Zicovich-Wilson and Dovesi carried out periodic Hartree–Fock calculations on Ti-containing zeolites such as SOD, CHA, and alpha-quartz (QUA).[25] Interestingly, they showed that the substitution of Si atoms by Ti atoms in a zeolite is an endothermic process when evaluated with respect to pure silicozeolite. They also proved that the incorporation of Ti within the zeolite framework is thermodynamically less favored than the formation of extra-framework TiO_2 clusters. This explains the difficulty of synthesizing high Ti content zeolites.[25] Very recently, Damin et al. studied the interaction of Ti-CHA with various molecules such as NH_3, H_2O, H_2CO, and CH_3CN using a periodic approach.[33] Moreover, there have been several studies on other zeolites by using a periodic description.[34] Recently, Rozanska et al. have used a periodic approach to study the chemisorption of several organic molecules in zeolites.[35]

As discussed above, the Sn centers are catalytically very important and act as stronger Lewis acidic sites during the oxidation and reduction reactions. Thus, it is necessary to obtain the information on the structural and electronic properties of Sn-BEA. Motivated by this, in the present work, we examine the effect of the incorporation of Sn in BEA using a periodic model of this zeolite. Indeed, when the number of substituted Si atoms per unit cell is very small (here 1/64), the system can be assumed periodic.

Computational Methods

All the calculations presented in this paper were performed using the Vienna ab initio simulation package (VASP) code.[36] The instantaneous electronic ground state was calculated by solving the Kohn–Sham equation based on DFT. The periodic boundary condition was used to take care of the periodicity of the solid. The present method used the plane-wave basis set in conjunction with the ultra-soft Vanderbilt pseudopotentials.[37] The advantage of using this computationally efficient scheme is that it permits the use of fast Fourier transform techniques. The exchange correlation functional was expressed within the generalized gradient approximation (GGA) with the Perdew–Wang 91 functional.[38] The Brillouin zone sampling was restricted to the gamma point.

Structural relaxation of the coordinates of BEA and Sn-BEA was performed in two steps. Initially, the conjugate gradient method was employed to optimize the structures, during which the cell shape of the unit cell was fully relaxed by keeping the volume fixed. This was done until the forces on the atoms were less than 0.1 eVA^{-1}. In the next step the optimized structure obtained from the conjugate gradient was used as the starting geometry and was re-optimized by using the quasi-Newton method (volume fixed), unless the forces on the atoms were less than 0.06 eVA^{-1}. BEA has nine inequivalent X-ray crystallographically defined T-sites.[31] During the Sn-BEA unit cell optimization, all these nine T-sites were substituted one by one by Sn atoms, such that only one Sn atom was present per unit cell, that is, Si/Sn = 63/1. The unit cell was also optimized with two Sn atoms per unit cell as described above, that is,

Si/Sn = 62/2. In this optimization, the two Sn atoms were substituted at the two T9 sites.

Results and Discussion

Structure: The optimized structural parameters of Sn-BEA for all the nine T-sites (T1 to T9) are given in Table 1. As discussed in the introduction, BEA has nine inequivalent X-ray crystallographically defined T-sites (Figure 1). There are basically 192 atoms in the unit cell with 64 Si atoms and 128 O atoms. The distribution of these 64 Si atoms is as follows: there are eight Si atoms placed at the T1–T6 and T8 positions, while four Si atoms are placed at the T7 and T9 positions. Only the average Sn–O, Sn–Si distances and Sn-O-Si bond angles are presented. The optimized average Si–O bond lengths and the Si-O-Si bond angles of BEA are 1.612 ± 0.002 Å and $149.25 \pm 1.5°$, respectively; these values are in good agreement with the earlier studies.[11] As expected, after the substitution of the Sn atom in the BEA, the average Sn–O bond lengths is 1.912 ± 0.002 Å and the bond angles range from 137 to 147°. This shows that, after replacing Si by Sn at the active sites in the BEA framework, the Sn–O bond length increases by about 0.3 Å with respect to the Si–O bond lengths, and the Sn-O-Si bond angles decrease by about 2–10° relative to the Si-O-Si bond angles. Although there is a decrease in the bond angle of the Sn-O-Si, the Sn–Si distance is more than the Si–Si distance in BEA; this difference is due to the increase in the Sn–O distance. It has been already confirmed by the experimental studies such as the ^{119}Sn MAS NMR spectroscopy, that the Sn atoms in the Sn-BEA are situated in the framework with tetrahedral coordination.[8,22–24] The O-Sn-O angles have also been calculated and it was seen that each of the angles significantly deviates from the tetrahedral value. These kind of O-T-O angle deviations from the tetrahedral values are also reported for the titanosilica zeolite models.[25] However, the average of all the O-Sn-O bond angles is close to 109.5°. Unfortunately, there are no earlier theoretical studies on Sn-BEA to compare with the results presented in this work. The change in the bonding due to the distortion in the the local Sn site of Sn-BEA is discussed in the next section. We observe from Table 1, that the T2 and the T8 positions have the shortest Sn–O bond lengths of 1.909 and 1.908 Å, respectively. However, the bond angle of the Sn-O-Si at the T2 position is the largest with 144.2°. The Sn–Si distance is the largest for T2 position, which can be attributed to the larger Sn-O-Si bond angle. The T4 position has the largest Sn–O bond length of about 1.917 Å and the smallest Sn-O-Si bond angle of 136.0°. The change in the structural parameters of each T-site can drastically affect the energetics of the zeolite. Hence, the stability and the reactivity of each site would be different.

Table 1. Average Sn–O bond lengths [Å] and Sn-O-Si bond angles, and the next nearest neighbor Sn–Si distance [Å] of the optimized structures for the nine different T-sites in Sn-BEA.

	Sn–O	Sn-O-Si	Sn–Si
T1	1.911	143.5	3.336
T2	1.909	144.2	3.341
T3	1.910	140.6	3.241
T4	1.917	136.0	3.281
T5	1.913	142.2	3.297
T6	1.910	141.2	3.297
T7	1.911	140.6	3.282
T8	1.908	140.0	3.282
T9	1.912	137.8	3.270

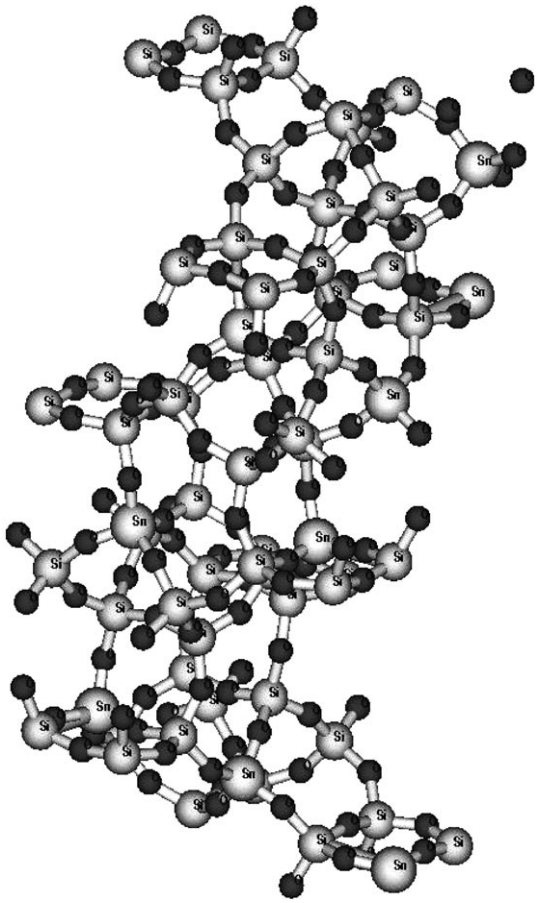

Figure 1. Unit cell of BEA consisting of 192 atoms. The nine active sites are shown by the Sn atoms (big grey spheres). The other are the Si (small gray spheres) and the O (black spheres) atoms.

Relative cohesive energy and stability: In this subsection we discuss the relative cohesive energies and hence the stabilities of all the nine substituted Sn sites. The cohesive energies for all nine T sites are given in Table 2. The cohesive energy is the difference between the energy of the bulk (solid) at equilibrium and the energy of the constituent atoms in their ground state. Hence, in the present study the cohesive energy can be taken as a measure of the stability with respect to the decomposition. The cohesive energy is given in Equation (1) in which i represents the individual atoms that constitute the solid.

Table 2. Cohesive energies, HOMO and LUMO energies, and the HOMO–LUMO gap of the nine different T-sites.

	Cohesive energy [eV]	HOMO energy [eV]	LUMO energy [eV]	HOMO–LUMO gap [eV]
T1	−1521.3871	−3.124	1.333	4.457
T2	−1521.6818	−3.125	1.366	4.491
T3	−1521.4687	−3.131	1.557	4.688
T4	−1521.5232	−3.117	1.421	4.538
T5	−1521.4052	−3.131	1.450	4.581
T6	−1521.4316	−3.120	1.426	4.546
T7	−1521.4571	−3.121	1.419	4.540
T8	−1521.6215	−3.117	1.497	4.614
T9	−1521.3239	−3.114	1.506	4.620

$$E_{coh} = E_{solid} - \sum_i E_i \quad (1)$$

The higher the cohesive energy of the solid, the more stable it is and more energy is required to decompose the solid. The cohesive energy of a fully siliceous BEA is −1527.9026 eV. From Table 2, we see that the cohesive energy of Sn-BEA ranges between −1521.32 and −1521.68 eV, which is about ~6 eV lower than the BEA. This explains the fact that the substitution of Sn in the BEA framework decreases the cohesive energy. To confirm this, we performed an optimization of Sn-BEA with two Sn atoms in the unit cell and it was seen that the cohesive energy decreases by about 6 eV (138 kcal mol^{-1}) relative to the case with one Sn atom in the unit cell. It has been shown by experiment that the turnover number and selectivity of cyclohexanone the Baeyer–Villiger reaction decreases with increase in the Sn content in the framework.[8,22–24] Very interestingly, we can say that the decrease in the cohesive energy of Sn-BEA with increase in the Sn content affects the turnover number and selectivity of cyclohexanone in the Baeyer–Villiger oxidation reaction. This kind of experimental evidence was provided for Ti content in TS-1.[39] However, more discussion is needed to understand this issue.

Among the nine T-sites, the T2 site has the highest cohesive energy (Table 2), and hence shows the most stable site for the substitution of Sn atom in Sn-BEA. This can also be attributed to the shorter Sn−O distance and longer Sn-O-Si bond angle. The next most stable site is the T8 site, which has ~0.06 eV (~1.5 kcal mol^{-1}) less cohesive energy than the T2 site. One should note that, the difference in the cohesive energy of the T2 and the T8 site is very little. Hence, in a kinetic controlled synthesis one cannot predict the most probable site between the T2 and T8 sites. The most unstable site is the T9 site which has ~0.35 eV (~8.23 kcal mol^{-1}) less energy than the T2 site (Table 2).

LUMO energies: It has been known that, lower the LUMO energy of a system, the higher is its ability to gain electron density and, hence, has a higher Lewis acidity. Sastre and Corma used the LUMO energies to characterize the Lewis acidity of the Ti sites in Ti-BEA and TS-1.[31] They showed that the average LUMO energy of the Ti sites in Ti-beta is lower than that in TS-1 and, hence, Ti-beta was shown to have a higher Lewis acidity than TS-1. On this basis, in the present work we use the LUMO energies to discuss the Lewis acidity of all nine T-sites in Sn-BEA. The highest occupied molecular orbital (HOMO) energies, LUMO energies, and the HOMO–LUMO gap of all nine T-sites are given in Table 2. The results show that the T1 and the T2 sites in Sn-BEA have the lowest LUMO energies and should be the most probable Lewis acid sites. It is worth mentioning that the reason for this would be their association to one four-membered ring as discussed by Valerio et al.[17] One should note that LUMO energies only decide the strength of the Lewis acidity of a particular T site and, hence, a favorable site for a oxidation reaction. It can also be said that the cohesive energy and the LUMO energy together decide the most favorable site for the substitution and reaction, respectively. Hence, on the account of high cohesive energy and low LUMO energy, the T2 site would be the most probable site for the substitution for the Sn atom and for the oxidation reactioin in Sn-BEA, if the most stable site of the dehydrated zeolite is also the most favorable for Sn incorporation at the synthesis conditions. We can also see that the HOMO–LUMO gap of the T1 and T2 sites is the smaleest; therefore these would be the most reactive sites.

The LUMO energy calculated for BEA is 2.643 eV, which is about 1.2–1.3 eV higher than the Sn-BEA (Table 2). These values indicate that the substitution of Sn in BEA drastically increases the Lewis acidity.

Bonding: In this subsection we focus on the nature of bonding in the Sn-BEA and compare this to the same in BEA. In Figures 2 and 3 the HOMO and the LUMO isodensities, respectively, of BEA at one third of the maximum isosurface value are plotted. We can clearly see that the HOMO of BEA indicates a p orbital on the oxygen atom. The LUMO isodensities of BEA (Figure 3) only show electron localization on the oxygen atoms, but no bond formation.

Figures 4 and 5 show the respective HOMO and LUMO isodensities of the Sn-BEA at one third of the maximum isosurface value. The HOMO isodensity of Sn-BEA is different from Si-BEA, which does not show any p orbital on oxygen atoms attached to the Sn atom (Figure 4), as seen in Si-BEA. Interestingly, the LUMO isodensity of Sn-BEA shows that the lone pair of electrons on the oxygen atoms coordinated to the Sn atom are polarized by the Sn atom (Figure 5), which is not seen in the LUMO of Si-BEA. This polarization of the electron density along the Sn−O bond can be attributed to the high Lewis acidity of the Sn atom.

Conclusion

In the present work we have discussed the structure, bonding, and acidity of the Sn-substituted BEA by using a periodic approach based on density functional theory. The results demonstrate that the incorporation of Sn in the BEA framework decreases the cohesive energy and is an endo-

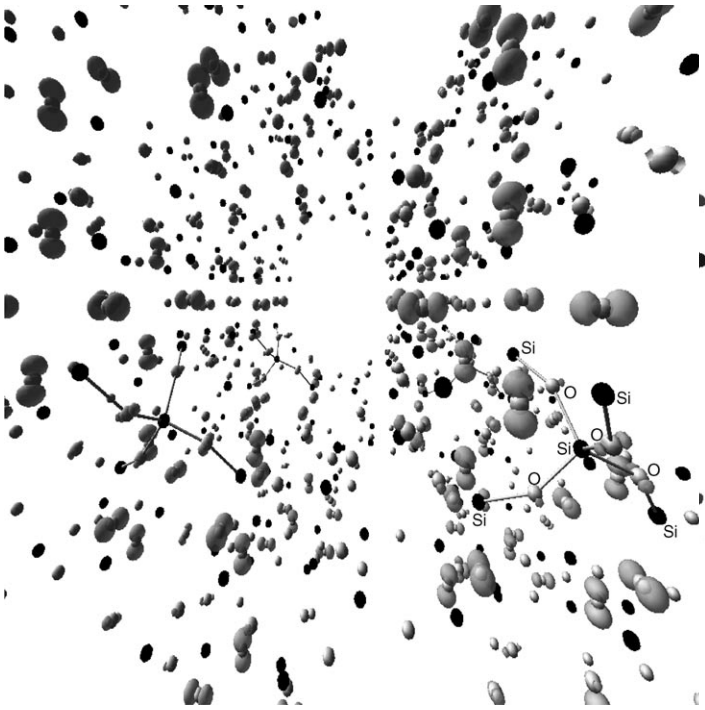

Figure 2. Isosurface of HOMO of BEA. Black and gray spheres are the Si and O atoms, respectively.

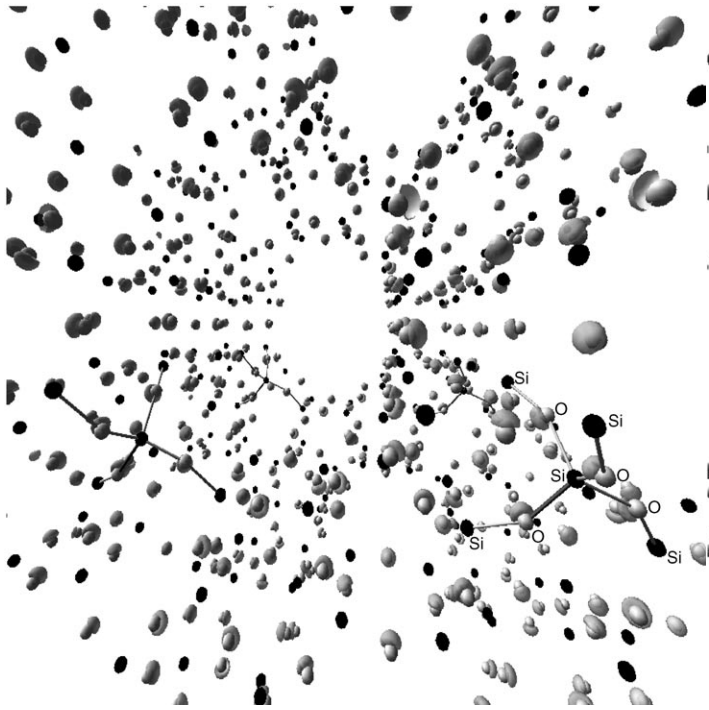

Figure 3. Isosurface of LUMO of BEA. Black and gray spheres are the Si and O atoms, respectively.

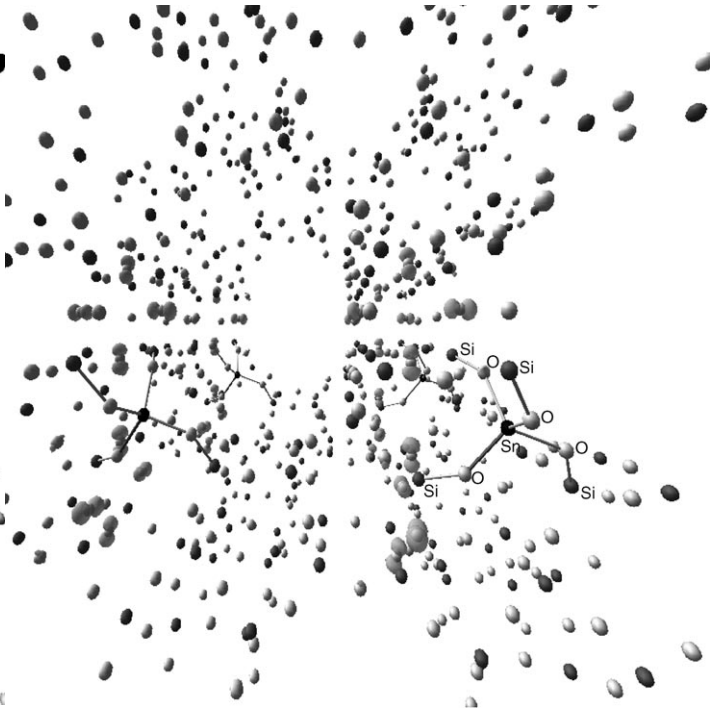

Figure 4. Isosurface of HOMO of Sn-BEA. Dark and light gray spheres are the Si and O atoms, respectively, and the Sn atom is shown by the black sphere.

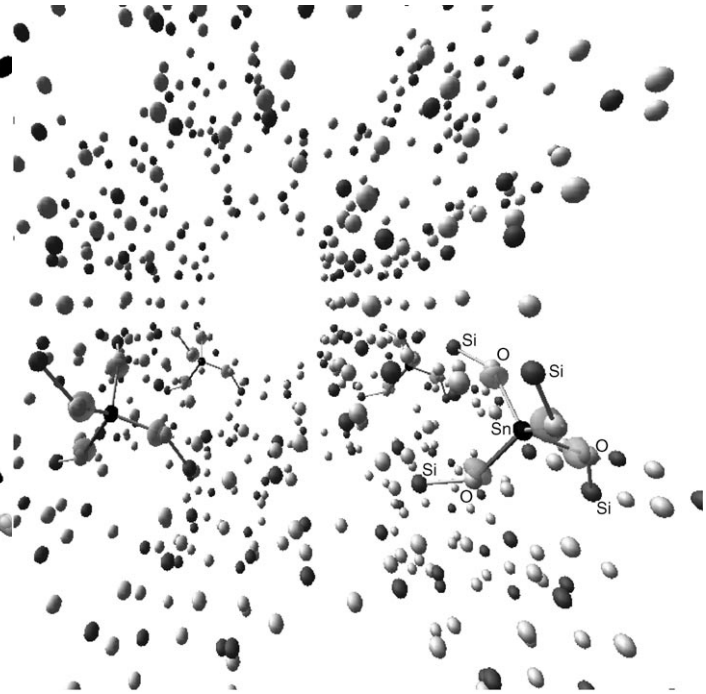

Figure 5. Isosurface of LUMO of Sn-BEA. Dark and light gray spheres are the Si and O atoms, respectively, and the Sn atom is shown by the black sphere.

thermic process. Hence, it is clear that the incorporation of Sn in the BEA is limited. This would be the reason for the decrease in the turnover number as the Sn content is increased in BEA during the Baeyer–Villiger oxidation reaction. The structural parameters, as expected, show longer Sn–O bond lengths relative to the Si–O bond lengths in BEA. Among the nine T-sites, the T2 site proves to be the

most stable site for the substitution of Sn in the BEA framework; this stability is due to the higher cohesive energy relative to the other T sites. Moreover, the T2 site is a higher Lewis acidic site relative to the other T-sites. The bonding analysis is necessary for a qualitative description of the electronegativity of Sn in Sn-BEA with respect to Si-BEA. The analysis shows that the Sn atom in Sn-BEA polarizes the orbital of oxygen atoms, which can be attributed to its higher electronegativity and, hence, higher Lewis acidity, confirming the quantitative results.

The present theoretical study gives an insight into the structural and the electronic properties of the T sites in Sn-BEA which is otherwise difficult by using the experimental techniques. Further work on the effect of solvent molecules on the Sn sites is still in progress.

Acknowledgements

S.S., S.P., and A.G. gratefully acknowledge the Indo–French Center for the Promotion of Advance Research (IFCPAR) (Project. No. 2605–2), New Delhi (India), for financial assistance.

[1] R. L Wadlinger, G. T. Kerr, E. J. Rosinski, US Pat. 3308069, **1967**.
[2] J. M. Newsam, M. M. J. Treacy, W. T. Koestsier, C. B. de Gruyter, *Proc. R. Soc. London Ser. A* **1988**, *420*, 375–405.
[3] a) A. Corma, M. T. Navarro, F. Rey, J. Rius, S. Valencia, *Angew. Chem.* **2001**, *113*, 2337–2340; *Angew. Chem. Int. Ed.* **2001**, *40*, 2277–2280; b) A. Corma, M. T. Navarro, F. Rey, S. Valencia, *Chem. Commun.* **2001**, 1486–1487; c) T. Ohusna, Z. Liu, O. Terasaki, K. Hiraga, M. A. Camblor, *J. Phys. Chem. B* **2002**, *106*, 5673–5678.
[4] a) J. A. Martens, J. Perez-Pariente, E. Sastre, A. Corma, P. A. Jacobs, *Appl. Catal.* **1988**, *45*, 85–101; b) P. Ratnasamy, R. N. Bhat, S. K. Pokhriyal, S. G. Hagde, R. Kumar, *J. Catal.* **1989**, *119*, 65–70; c) K. S. N. Reddy, M. J. Eapen, H. S. Soni, P. V. Shiralkar, *J. Phys. Chem.* **1992**, *96*, 7923–7928.
[5] G. Bellusi, G. Pazzuconi, C. Perego, G. Girotti, G. Terzoni, *J. Catal.* **1995**, *157*, 227–234.
[6] L. Bonetto, M. A. Camblor, A. Corma, J. Perez-Pariente, *Appl. Catal. A* **1992**, *82*, 37–50.
[7] a) A. J. Hoefnagel, H. van Bekkum, *Appl. Catal. A* **1993**, *97*, 87–102; b) K. P. de Jong, C. M. A. M. Mesters, D. G. R. Peferoen, P. T. M. van Brugge, C. de Groot, *Chem. Eng. Sci.* **1996**, *51*, 2053–2060.
[8] A. Corma, L. T. Nemeth, M. Renz, S. Valencia, *Nature* **2001**, *412*, 423–425.
[9] M. A. Camblor, A. Corma, A. Martinez, J. Perez-Pariente, *J. Chem. Soc. Chem. Commun.* **1992**, 589–590.
[10] T. Sen, M. Chatterjee, S. J. Sivsanker, *Chem. Soc. Chem. Commun.* **1995**, 207–208.
[11] J. C. van der Waal, H. van Bekkum, *J. Mol. Catal. A* **1997**, *124*, 137–146.
[12] M. A. Camblor, A. Corma, J. Perez-Pariente, *Zeolites* **1993**, *13*, 82–87.
[13] J. C. Jansen, E. J. Creyghton, S. L. Njo, H. van Koningsveld, H. van Bekkum, *Catal. Today* **1997**, *38*, 205–212.
[14] A. Corma, M. H. Camblor, P. Esteve, A. Martinez, J. Perez-Pariente, *J. Catal.* **1994**, *145*, 151–158.
[15] A. Corma, P. Esteve, A. Martinez, S. Valencia, *J. Catal.* **1995**, *152*, 18–24.
[16] L. C. de Menorval, W. Buckermann, F. Figueras, F. Fajula, *J. Phys. Chem.* **1996**, *100*, 465–467.
[17] G. Valerio, A. Goursot, R. Vetrivel, O. Malkina, V. Malkina, D. R. Salahub, *J. Am. Chem. Soc.* **1998**, *120*, 11426–11431.
[18] A. Corma, P. Esteve, A. Martinez, *Zeolites* **1996**, *16*, 7–14.
[19] A. Carati, C. Flego, E. Previde Massara, R. Millini, L. Carluccio, N. D. Parker, Jr., G. Bellussi, *Microporous Mesoporous Mater.* **1999**, *30*, 137–144.
[20] W. Adam, H. Garcia, C. M. Mitchell, C. R. Saha-Mollera, O. Weichold, *Chem. Commun.* **1998**, 2609–2610.
[21] N. K. Mal, A. V. Ramaswamy, *Chem. Commun.* **1997**, 425–426.
[22] A. Corma, M. E. Domine, L. Nemeth, S. Valencia, *J. Am. Chem. Soc.* **2002**, *124*, 3194–3195.
[23] A. Corma, M. E. Domine, S. Valencia, *J. Catal.* **2003**, *215*, 294–304.
[24] M. Renz, T. Blasco, A. Corma, V. Formes, R. Jensen, L. Nemeth, *Chem. Eur. J.* **2002**, *8*, 4708–4717.
[25] C. M. Zicovich-Wilson, R. Dovesi, *J. Phys. Chem. B* **1998**, *102*, 1411–1417.
[26] T. Blasco, M. A. Camblor, A. Corma, J. Perez-Pariente, *J. Am. Chem. Soc.* **1993**, *115*, 11806–11813.
[27] T. Blasco, M. A. Camblor, A. Corma, P. Esteve, J. M. Guil, A. Martinez, J. A. Perdigon-Melon, S. Valencia, *J. Phys. Chem. B* **1998**, *102*, 75–88.
[28] J. Sauer, *Chem. Rev.* **1989**, *89*, 199–255.
[29] J. Sauer, P. Ugliengo, E. Garrone, V. R. Saunders, *Chem. Rev.* **1994**, *94*, 2095–2160.
[30] J-R. Hill, C. M. Freeman, B. Delley, *J. Phys. Chem. A* **1999**, *103*, 3772–3777.
[31] G. Sastre, A. Corma, *Chem. Phys. Lett.* **1999**, *302*, 447–453.
[32] R. Dimitrova, M. Popova, *Mol. Eng.* **1998**, *8*, 471–478.
[33] A. Damin, S. Bordiga, A. Zecchina, K. Doll, C. Lamberti, *J. Chem. Phys.* **2003**, *118*, 10183–10194.
[34] a) R. Shah, J. D. Gale, M. C. Payne, *J. Phys. Chem.* **1996**, *100*, 11688–11697; b) T. Demuth, J. Hafner, L. Benco, H. Toulhoat, *J. Phys. Chem. B* **2000**, *104*, 4593–4607.
[35] X. Rozanska, T. Demuth, F. Hutschka, J. Hafner, R. A. van Santen, *J. Phys. Chem. B* **2002**, *106*, 3248–3254.
[36] a) G. Kresse, J. Hafner, *Phys. Rev. B* **1994**, *49*, 14251–14269; b) G. Kresse, J. Furthmuller, *Comput. Mater. Sci.* **1996**, *6*, 15.
[37] D. Vanderbilt, *Phys. Rev. B* **1990**, *41*, 7892–7895.
[38] J. P. Perdew, Y. Wang, *Phys. Rev. B* **1992**, *45*, 13244–13249.
[39] B. Notari, *Adv. Catal.* **1996**, *41*, 253–334.

Received: May 2, 2005
Published online: September 27, 2005

